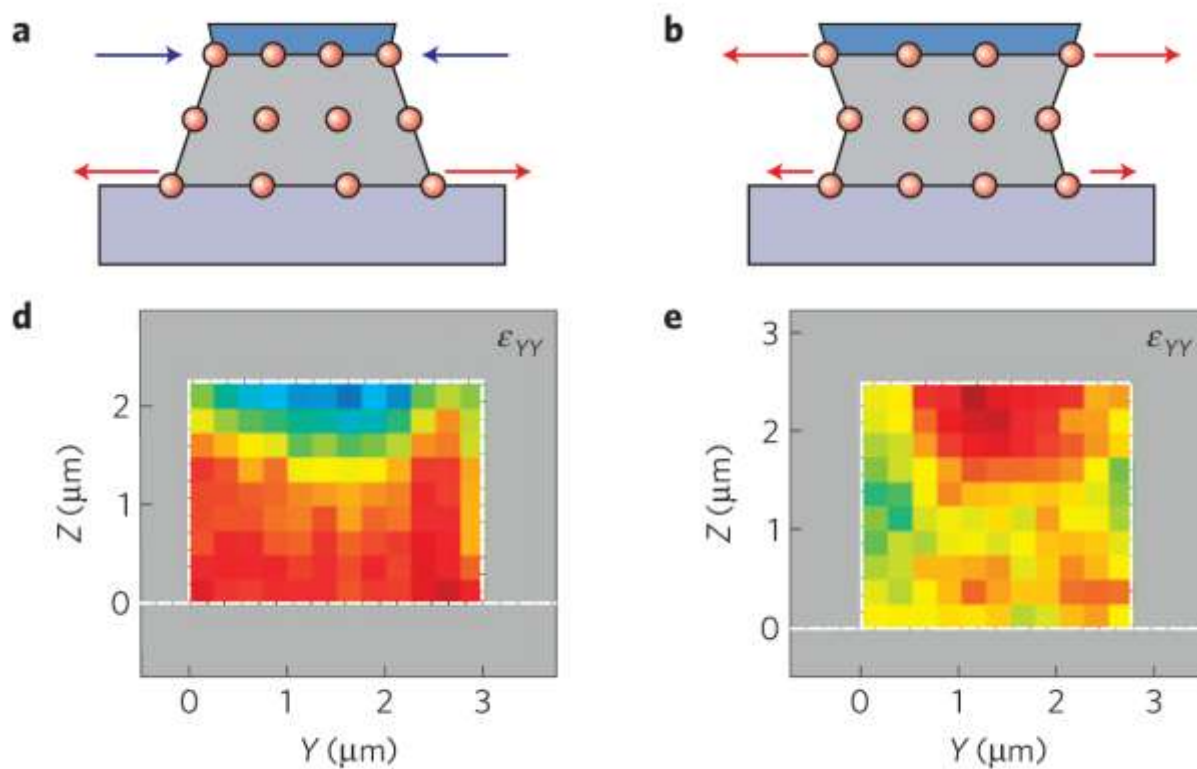


# NANOSCIENCE LABORATORY



## HIGHLIGHTS 2012

## NANOSCIENCE LABORATORY HIGHLIGHTS 2012

### MEMBERS (2012)

#### Faculty and research staff

Lorenzo Pavesi (full professor, head)  
Marina Scarpa (full professor)  
Zeno Gaburro (assistant professor)

#### Technical staff

Massimo Cazzanelli (EP2 level)  
Paolo Bettotti (EP1 level)  
Enrico Moser

#### Administrative staff

Tatsiana Yatskevich

#### Post-doctoral fellows

Oleksiy Anopchenko  
Elena Froner  
Philip Ingenhoven  
Kamil Fedus (left 1.2012)

Fernando Ramiro Manzano  
Francisco Aparicio Rebollo (left 9.2012)  
Nikola Prtljaga

#### Doctoral students

Mattia Mancinelli  
Federica Bianco  
Fabrizio Sgrignuoli  
Andrea Tengattini  
Neeraj Kumar  
Davide Gandolfi  
Massimo Borghi

#### Master students

Laura Cattoni  
Paolo Cortelletti  
Mattia Signoretto  
Andrea Zanzi

---

## SCIENTIFIC MISSION

### Introduction to the Nanoscience Laboratory

The Nanoscience Laboratory (NL) is a laboratory of the Physics Department with interests in nanophotonics, silicon-based photonics and nanobiotechnologies. Its mission is to generate new knowledge and understanding from physical phenomena which occur when the matter is of nanometer size. In particular, NL is trying to apply the nanoscience paradigm to silicon or silicon compatible materials to enable new application of this key material, and to develop nanosystems compatible with the main driving silicon technologies. However silicon is not the only material studied. Other projects concern the use of polymers to tailor the properties of nanostructure atom-by-atom or metals to investigate new properties which rise from plasmonics. A particular emphasis is placed on photonics and its applications. Research projects span from fundamental research work on the interaction between biomolecules and silicon nanostructures or on the control of photons by dynamically structuring the dielectric environment, to more applied research work on the development of integrated optical circuits, optical switches, light emitting devices and amplifiers, novel MIR and THz sources, third generation photovoltaic and biosensors.

NL is composed by more than 20 people with interdisciplinary scientific background. Researchers from physics, bio-chemistry, materials science and electrical engineering interact to form a group of interdisciplinary nature. They came from all around the world and the language spoken in the laboratory is English.

Of particular mention is the collaboration that NL has with the Center of Materials and Microsystems, in particular with the Advance Photonics and Photovoltaic and the Biofunctional Surfaces and Interfaces units, the Fondazione Bruno Kessler (FBK). The collaboration spans over the last twenty years and covers fabrication, testing and application of biomaterials and silicon based devices. Many common projects exist among which a project on the development of a multispectral protein chip for application in diagnostics (NAOMI, supported by Provincia Autonoma di Trento (PAT)).

NL, with the help of the local institutes of CNR and FBK, organizes each two years a winter school on optoelectronics and photonics; the 7<sup>th</sup> Photonics and Optoelectronics Winter School: Physics and Application of Optical Resonators, will be held from 16<sup>th</sup> till 22<sup>nd</sup> of March, 2013. Members of NL participate in the committee or organize several international conferences or workshop.

Research of NL is mainly funded by the local government (PAT), the European commission within the research frameworks, the MIUR and by companies. During the period covered by these Highlights, NL has been and is involved in the following projects: NAOMI (supported by

PAT), NANO@AT (supported by PAT within the collaboration between Adelaide & Trento), projects on the mid-wave infrared supercontinuum from silicon waveguides (supported by the CARIPLO foundation), collaborative project Italy-India (ITPAR) supported by MIUR, some European projects within the 7<sup>th</sup> Framework: HELIOS (FP7-ICT-224312), LIMA (FP7-ICT-248909), POSITIVE (FP7-ICT-257401), El-Dorado (FP7-PEOPLE-235860), APPCOPTOR (FP7-PEOPLE-275150).

### Silicon Nanophotonics

Silicon photonics is the technology where photonic devices are produced by standard microelectronic processes using the same paradigm of electronics: integration of a large number of devices to yield a high circuit complexity which allows for high performances and low costs. Here, the real truth is to develop photonic devices that can be easily integrated to improve the single device performance and to allow high volume production.

We are involved in researching new optical scheme for implementing optical network on a chip by using concepts of nanophotonics. We use the concept of whispering gallery modes which develops in micro-disks or micro-rings to further tune the photon mode density. These disks or rings are coupled directly with narrow mode SOI (Silicon-on-Insulator) waveguides. High quality factor cavities allow to study fundamental quantum optics concept such as optical forces. Series of coupled micro-rings are studied to implement novel scheme of phase controlled optical networks where EIT (electromagnetic induced transparency) is manifested and exploited to route optical signals.

To develop silicon photonics, one further add-on is making silicon do something which it is not able to do in its standard (bulk) form. Low dimensional silicon, where small silicon nanocrystals or nanoclusters (Si-nc) are developed, is one way to compel silicon to act as an active optical material. The key ingredient that makes Si-nc appealing for photonics are: quantum size effects which makes new phenomena appear in silicon, such as room temperature visible photoluminescence, optical gain, coulomb blockade and multiexciton generation. Our research interests are to exploit quantum confinement and reduced dimensionality to produce effective light sources, lasers, optical amplifiers. In addition, we use quantum confinement to increase the nonlinear optical properties of silicon and to achieve optical switching. Finally, the use of strain to tune the nonlinear optical properties of silicon waveguides paves the wave to the development of new MIR sources.

### Nanobiotechnologies, antioxidants and human health

All the aspects related to the nano-bio interfaces (which are the structures where the co-existence of physical principles and biological molecules is clearly evident) are a challenging field of research. Though the leading research concerns the design, synthesis and dynamic behavior of nano-structured bio-interfaces, more specifically we are working on three research topics: silicon- and titanium based nanosystems, single molecule detection, and antioxidant behavior in micelle systems.

To develop silicon based bio-sensors, we are currently focused on silicon based hybrid nanostructures. In particular

silicon or silicon nitride flat or porous films are the starting inorganic support into which bio active layers are designed. Biological recognition elements are introduced on this hybrid layer. Molecular surface density, active layer thickness and integration of the bio-active interface with photonic devices will be the future challenges to develop the sensor system. In addition, we are developing nanostructured hybrid interfaces to capture bio-analytes and enhance their Raman signals. Gold and silver nanoparticles are used as enhancers.

Beyond traditional sensor applications, silicon nanostructures can be used as “nanosensors”, which monitor the intracellular events without introducing irreversible perturbations. To this regard light emitting silicon quantum dots appear very promising. We are studying the nanoparticle coating to increase optical stability and decrease toxicity, moreover conjugation to biological molecules and strategies to increase cell uptake and control intracellular localization are future steps of this research. Titanium nanotubes showing hydroxyl-rich interfaces have been synthesized. These nanosystems are easily dispersed and stable in aqueous solutions and show a high photocatalytic activity. Antioxidant compounds are able to control reactive and damaging forms of oxygen, referred to as free radicals. Though antioxidants have been largely studied, much remains unknown about the human body adsorption and use of these compounds. We are investigating the synergistic effect of plasma antioxidants at the interface of micelle systems. Beyond the basic biophysical investigation, the crucial point is the development of devices and methodologies to monitor the antioxidant action. Being these processes free-radical mediated, a very high detection sensitivity is required. Moreover, to have physiological significance, the experiments should be performed in heterogeneous systems mimicking an un-perturbed biological environment. Thus we are proposing a new theoretically based methodology to compute antioxidant capacity and efficiency starting from oxygen concentration measurement, as well as, we are designing a nanostructured electrode to monitor molecular oxygen in real time.

### Experimental facilities

The NL facilities allow for detailed experimental studies in nanoscience, photonics and biotechnologies. Since the effective collaboration with FBK most material processing and device productions are performed within their premises.

For photonics, we have facilities to cover the light spectrum from the THz to UV ranges with whatever time resolution is needed. Laser sources comprehends: Ti-sapphire fs-ps laser (1 W average over 1000-700 nm, 2 ps or 70 fs pulses, 82 MHz repetition rate) interfaced with a second harmonic generator and pulse picker; Nd-Yag laser interfaced with an optical parametric oscillator which allows scanning the 400-3000 nm wavelength region (pulse 50 mJ, 10 ns, 10 Hz); TOPAS pumped with an amplified Ti:Sa laser which covers the 1-2.6  $\mu\text{m}$  range with 35 fs, 10 kHz, 3 mJ; one CW, UV extended, Ar laser; three tunable CW lasers (850-870 nm, 1200 - 1700 nm and 1500 - 1600nm) fiber pig-tailed; 4W EDFA and 2W semiconductor amplifiers, several pig-tailed diode lasers, ASE source

at 1550 nm and a broad band SLD at 800 nm. Three high-power true-CW DPSS single-line laser operating at 532, 473 and 355 nm. Detectors comprehend: visible and infrared photomultipliers and CCDs, a streak camera with ps resolution, 4K cooled bolometers which cover THz region, avalanche photodiodes for vis and IR ranges plus one capable of photon-counting in the third telecom window. To perform spectral analysis several set-ups are available: FTIR and dispersive spectrophotometers, a micro-Raman setup, a micro-FTIR and a UV-vis-IR spectrophotometer (shared with other laboratories), UV-Vis and fluorescence spectrophotometer dedicated to biochemical experiments. Five dedicated apparatus for WG characterization equipped with nanopositioning systems and polarization controllers are available, each one specified on a given functions: visible, infrared, pump-probe, grating coupling and non-linear measurements. Other apparatus are: - visible and infrared photoconductivity set-up; - a solar simulator for cell sizes up to 5 inches; - two nanoprobe stations (AFM and SNOM) - two semiconductor probe stations (4 and 8 inches) and many different electrical characterization set-ups (I-V, Z- $\omega$ , EL-I, etc.). Two VIS to NIR optical spectrum analyzers are available to NL-Lab. A probe station is fiber-bunch interfaced with a spectrometer interfaced with IR and visible liquid nitrogen cooled CCDs. For sample treatment and high sensitivity analytical detection, an electrochemical laboratory equipped with several chemical hots, spinners, galvanostates and voltmeters is available. An electron beam lithography set-up (SEM attachment) is also owned. For optical, electrical and molecular dynamic simulations, the laboratory uses free and commercial software, a dedicated cluster with 16 nodes and work-stations. Two laboratories, one dedicated to chemical synthesis and the second to biological sample preparation, are also available.

### 2012 PhD Thesis

Nikola Prtljaga "*Silicon nanocrystals: from bio-imager to Erbium sensitizers*" (30 march 2012)

### 2012 publications

1. "Second-harmonic generation in silicon waveguides strained by silicon nitride", M. Cazzanelli, F. Bianco, E. Borga, G. Pucker, M. Ghulinyan, E. Degoli, E. Luppi, V. Veniard, S. Ossicini, D. Modotto, S. Wabnitz, R. Pierobon, L. Pavesi, *Nature Materials*, 11, 148 (2012)
2. "Electrical pump & probe and injected carrier losses quantification in Er doped Si slot waveguides", J. M. Ramirez, Y. Berencen, F. Ferrarese Lupi, D. Navarro-Urrios, A. Anopchenko, A. Tengattini, N. Prtljaga, L. Pavesi, P. Rivallin, J. M. Fedeli, B. Garrido, *Opt. Express*, 20, 28808 (2012)
3. "Packing Confined Hard Spheres Denser with Adaptive Prism Phases", E. C. Oguz, M. Marechal, F. Ramiro-Manzano, I. Rodriguez, R. Messina, F. J. Meseguer, H. Lowen, *Phys. Rev. Lett.*, 109, 218301 (2012)
4. "Optimizing Picene Molecular Assembling by Supersonic Molecular Beam Deposition", S. Gottardi, T. Toccoli, S. Iannotta, P. Bettotti, A. Cassinese, M. Bara, L. Ricciotti, Y. Kubozono, *J. Phys. Chem. C*, 116, 245503 (2012)
5. "Reconfigurable optical routers based on Coupled Resonator Induced Transparency resonances", M. Mancinelli, P. Bettotti, J.M. Fedeli, L. Pavesi, *Opt. Express*, 20, 23856 (2012)
6. "A fully integrated high-Q Whispering-Gallery Wedge Resonator", F. Ramiro-Manzano, N. Prtljaga, L. Pavesi, G. Pucker, M. Ghulinyan, *Opt. Express*, 20, 22934 (2012)
7. "Limit to the erbium ions emission in silicon-rich oxide films by erbium ion clustering", N. Prtljaga, D. Navarro-Urrios, A. Tengattini, A. Anopchenko, J. M. Ramirez, J. M. Rebled, S. Estrade, J.-P. Colonna, J.-M. Fedeli, B. Garrido, L. Pavesi, *Opt. Mat. Express*, 2, 1278 (2012)
8. "Polarization strategies to improve the emission of Si-based light sources emitting at 1.55  $\mu\text{m}$ ", J.M. Ramirez, O. Jambois, Y. Berencen, D. Navarro-Urrios, A. Anopchenko, A. Marconi, N. Prtljaga, N. Daldosso, L. Pavesi, J.-P. Colonna, J.-M. Fedeli, B. Garrido, *Mater. Sci. Eng. B-Adv.*, 177, 734 (2012)
9. "Phase-Sensitive Detection for Optical Sensing With Porous Silicon", J. Alvarez, N. Kumar, P. Bettotti, D. Hill, J. Martanez-Pastor, *IEEE Photonics J.*, 4, 986 (2012)
10. "Two-dimensional micro-Raman mapping of stress and strain distributions in strained silicon waveguides", F. Bianco, K. Fedus, F. Enrichi, R. Pierobon, M. Cazzanelli, M. Ghulinyan, G. Pucker, L. Pavesi, *Semicond. Sci. Technol.*, 27, 085009 (2012)
11. "Light Combining for Interferometric Switching", M. Masi, M. Mancinelli, P. Bettotti, L. Pavesi, *Int. J. Optics*, 2012, Article ID 130517 (2012)
12. "Silicon nanocluster sensitization of erbium ions under low-energy optical excitation", N. Prtljaga, D. Navarro-Urrios, A. Pitanti, F. Ferrarese-Lupi, Blas Garrido, L. Pavesi, *J. Appl. Phys.*, 111, 094314 (2012)
13. "Bipolar pulsed excitation of erbium-doped nanosilicon light emitting diodes", A. Anopchenko, A. Tengattini, A. Marconi, N. Prtljaga, J. M. Ramirez, O. Jambois, Y. Berencen, D. Navarro-Urrios, B. Garrido, F. Milesi, J. P. Colonna, J. M. Fedeli, L. Pavesi, *J. Appl. Phys.*, 111, 063102 (2012)
14. "Optical and electrical properties of undoped and doped Ge nanocrystals", S. Das, R. Aluguri, S. Manna, R. K. Singha, A. Dhar, L. Pavesi, S. K. Ray, *Nanoscale Research Letters*, 7, 143 (2012)
15. "Erbium emission in MOS light emitting devices: from energy transfer to direct impact excitation", J. M. Ramirez, F. Ferrarese Lupi, O. Jambois, Y. Berencen, D. Navarro-Urrios, A. Anopchenko, A. Marconi, N. Prtljaga, A. Tengattini, L. Pavesi, J. P. Colonna, J. M. Fedeli, B. Garrido, *Nanotechnology* 23, 125203 (2012)
16. "Modeling of silicon nanocrystals based down-shifter for enhanced silicon solar cell performance", F. Sgrignuoli, G. Paternoster, A. Marconi, P. Ingenhoven, A. Anopchenko, G. Pucker, L. Pavesi, *J. Appl. Phys.*, 111, 034303 (2012)
17. "Photophysics of resonantly and non-resonantly excit-

- ed erbium doped Ge nanowires", S. Manna, N. Prtljaga, S. Das, N. Daldosso, S. K. Ray, L. Pavesi, *Nanotechnology*, 23, 065702 (2012)
18. "Effect of the annealing treatments on the electroluminescence efficiency of SiO<sub>2</sub> layers doped with Si and Er", O. Jambois, J. M. Ramirez, Y. Berencen, D. Navarro-Urrios, A. Anopchenko, A. Marconi, N. Prtljaga, A. Tengattini, P. Pellegrino, N. Daldosso, L. Pavesi, J.-P. Colonna, J.-M. Fedeli, B. Garrido, *J. Phys. D*, 45, 045103 (2012)
  19. "Silicon based monolithically integrated whispering gallery mode resonators with buried waveguides" M. Ghulinyan, F. Ramiro Manzano, R. Guiger, N. Prtljaga, G. Pucker and L. Pavesi, *Proc. of SPIE* 8431, 843110 (2012)
  20. "Opto-Electrical Characterization of Erbium Doped Slot Waveguides" Andrea Tengattini, Davide Gandolfi, Alessandro Marconi, Aleksei Anopchenko, Nikola Prtljaga, Joan Manel Ramirez, Federico Ferrarese Lupi, Yonder Berencen, Daniel Navarro Urrios, Blas Garrido, Jean-Marc Fedeli, Pierrette Rivallin, Kavita Surana, and Lorenzo Pavesi, *Proc. SPIE* 8431, 843118 (2012)
  21. "A Polarimetric sensor based on nanoporous free standing membranes" P. Bettotti, N. Kumar, L. Pavesi, J. Alvarez, D. Hill, *Proceedings of IEEE sensors* 6411315 (2012).
  22. "Cost model developed in European project LIMA", M.A. Vasquez, V. D. Mihailetchi, J. P. Connolly, O. Cubero, G. Daly, A. Halm, R. Kopecek, E. Perez, G. Pucker, G. Sanchez, L. Pavesi, *Energy Procedia* 27, 646-651 (2012).
  23. "La Nanofotonica in Silicio e la Fotonica con il Nanosilicio - Una piattaforma per ampliare il successo della fotonica in silicio" Aleksey Anopchenko, Francisco Javier Aparicio Rebollo, Paolo Bettotti, Federica Bianco, Pierluigi Bellutti, Massimo Cazzanelli, Kamil Fedus, Elena Froner, D. Gandolfi, Mher Ghulinyan, Neeraj Kumar, Yoann Jestin, Philip Ingenhoven, Silvia Larcheri, Lorenzo Lunelli, Mattia Mancinelli, Alessandro Marconi, Enrico Moser, Laura Pasquardini, Cecilia Pederzoli, Cristina Potrich, Nikola Prtljaga, Georg Pucker, Fernando Ramiro Manzano, Eveline Rigo, Marina Scarpa, Fabrizio Sgrignuoli, Andrea Tengattini, and Lorenzo Pavesi, *Il Nuovo Saggiatore*, vol 28 no 1-2 ) (2012) 5-15
  24. "Innovative Quantum Effects in Silicon for photovoltaic applications" Zhizhong Yuan, Aleksei Anopchenko, Lorenzo Pavesi, chapter 10, pag. 355-391 in *Advanced Silicon Materials for Photovoltaic Applications* edited by Sergio Pizzini (John Wiley and Sons Ltd, 2012)
  25. *Silicon Photonics and Photonic Integrated Circuits III*, special issue editors Laurent Vivien, Seppo K. Honkanen, Lorenzo Pavesi, Stefano Pelli, *Proceedings of the SPIE*, Volume 8431 May 2012

## 1. Limit to the erbium ions emission in silicon-rich oxide films by erbium ion clustering (Nikola Prtljaga)

Erbium ( $\text{Er}^{3+}$ )-doped silicon rich oxide (SRO) films are studied as active material to a silicon integrated optical amplifier or laser. By using the sensitization action of silicon nanoclusters (Si-ncl), limitations of the  $\text{Er}^{3+}$  excitation process are avoided (small absorption cross-section, spectrally narrow absorption lines), and the overall material emission performance is improved. At the same time, complementary-metal-oxide-semiconductor (CMOS) process compatibility is maintained, and emission in the third telecom window ( $1.53 \mu\text{m}$ ) is achieved. This allows for direct compatibility with the main stream semiconductor technology, which yields mass manufacturing and heavy integration density of photonic devices. Additional attractiveness is given by the possibility of electrical injection through electrical transport in the Si-ncl.

Despite these premises, optical gain achievement is still eluding. There is consensus in the literature that the principal reason obstructing the optical gain achievement in this material is a low fraction of sensitized erbium ions. Recently, we have demonstrated that this is followed by the loss of light emission capability of  $\text{Er}^{3+}$  when embedded in SRO material

[1]. While the main fraction of embedded erbium ions does not participate in the process of light emission, absorption properties of non-emitting ions remain unaltered [2]. Evidently, this becomes a major obstacle toward population inversion in this material. At this point, elucidating the origin of this phenomenon becomes of paramount significance for further material optimization and device development.

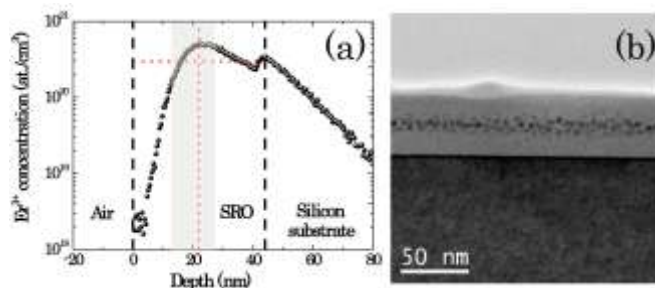


Figure 1. (a) Semi-log plot of erbium concentration profile in the studied samples obtained by SIMS. Thick vertical dashed lines indicate interfaces between air/SRO and SRO/silicon substrate. Vertical red dotted line corresponds to the peak  $\text{Er}^{3+}$  concentration, and the horizontal red dotted line to an average  $\text{Er}^{3+}$  concentration in the active layer. The shaded area corresponds to the layer where erbium clusters are visible in TEM images. (b) Bright field scanning TEM (STEM) image of the sample. Erbium clusters are visible as a dark spotted layer

In our work [1], we address this issue in a conclusive way and report on the mechanism responsible for it, i.e., erbium ion clustering. We have fabricated a series of thin ( $\sim 50$  nm) erbium-doped (by ion implantation) silicon-rich oxide films in the configuration that mitigates previously proposed mechanisms for loss of light emission capability of erbium ions. By combining the methods of optical, struc-

tural and electrical analysis, we identify the erbium ion clustering as a driving mechanism to low optical performance of this material. Experimental findings in this work clearly evidence inadequacy of the commonly employed optimization procedure when optical amplification is considered. We reveal that the significantly lower erbium ion concentrations are to be used in order to fully exploit the potential of this approach and achieve net optical gain.

### References:

1. N. Prtljaga, D. Navarro-Urrios, A. Tengattini, A. Anopchenko, J. M. Ramirez, J. M. Rebled, S. Estrade, J.-P. Colonna, J.-M. Fedeli, B. Garrido, L. Pavesi, "Limit to the erbium ions emission in silicon-rich oxide films by erbium ion clustering", *Opt. Mat. Express*, 2, 1278 (2012)

## 2. Towards a $1.54 \mu\text{m}$ electrically driven Erbium doped Silicon Optical Amplifier (Andrea Tengattini)

Erbium-doped silicon-rich-silicon oxide (SRO) films could offer a promising material platform for the development of compact waveguide amplifiers and lasers. The most important advantage of this approach is given by the possibility to have efficient electrical injection of Er ions [1]. In order to have an efficient electrical injection, very thin films are required. In addition, multilayered SRO structures allow for bipolar direct tunneling. Slot waveguides, where light confinement happens in a thin low refractive index layer sandwiched by two thick high refractive index materials, emerge as a natural choice. In our laboratory, we have designed and modeled a new structure of an electrically driven Er doped silicon slot waveguides, and then we have characterized these devices fabricated in a standard complementary metal-oxide semiconductor (CMOS) fab line, in Grenoble. The figure 2 shows a top view optical image of the fabricated devices.

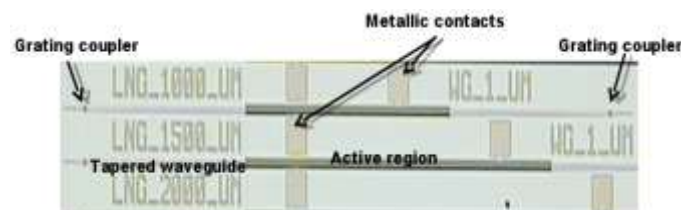


Figure 2. Top view optical image of the fabricated waveguides

Optical propagation losses have been evaluated by using waveguides with different lengths (1–3 mm). The propagation losses are in the order of  $(40 \pm 5)$  dB/cm in the region between 1500 and 1600 nm for both waveguide types [2]. No wavelength dependence is observed. On the other side, the electroluminescence (EL) spectrum evidences that we excite the Er ions by impact excitation caused by hot carrier injection. The voltage range, where the EL signal can be detected, is very small (only 10 V, voltages higher than 40 V). The optical power density collected is in the range of tens of  $\mu\text{W}/\text{cm}^2$ , which increases linearly with the electric field applied and superlinearly with the injected current [3]. The optical conversion efficiency, defined as the ratio between the output optical power and the forced electrical

power, is equal to  $10^{-4}$  %. Lastly, we test the transmission of a probe signal as a function of the applied voltage. This experiment could give insights on the suitability of this approach for an on-chip optical amplifier. The figure 3 shows the ratio between the transmitted signal at an applied bias  $U$  versus the transmitted signal for  $U = 0$  V — this quantity is usually reported in the literature as signal enhancement (SE). The reported data are for a probing signal wavelength of 1550 nm. We observed that the SE decreases for increased bias voltage. No dependence on the signal wavelength is observed too. We attribute this effect to charge accumulation in the silicon nanocrystals or in the defects in the oxide and to the free carrier absorption phenomenon, caused by the injected current in the silicon slot waveguide. The losses are higher in forward bias (negative voltage applied to the gate) than in the reverse one, because the injected electron current is higher, too.

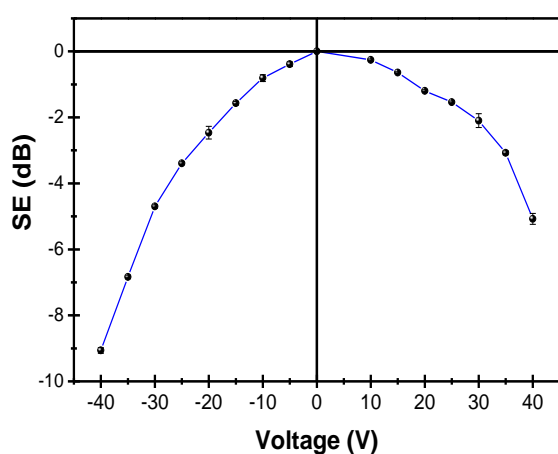


Figure 3. SE as a function of the applied voltage at a fixed probing wavelength of 1550 nm

These results suggest that the high propagation losses and the free carrier absorption phenomenon have to be reduced in order to make a working device. Lastly, erbium implanted silicon ring resonators coupled to slot waveguides have been designed and fabricated. Electro optical properties under electrical bias are under study, paving the way towards the possibility of building an electrically pumped silicon laser.

Work supported by FP7-HELIOS.

#### References:

1. A. Anopchenko, A. Tengattini, A. Marconi, N. Prtljaga, J. M. Ramírez, O. Jambois, Y. Berencén, D. Navarro-Urrios, B. Garrido, F. Milesi, J.-P. Colonna, J.-M. Fedeli, and L. Pavesi, "Bipolar Pulsed Excitation of Erbium-Doped Nanosilicon LEDs," *J. Appl. Phys.*, 111, 063102 (2012).
2. A. Tengattini, D. Gandolfi, A. Marconi, O. Anopchenko, N. Prtljaga, J. M. Ramirez, F. F. Lupi, Y. Berencen, D. Navarro Urrios, B. Garrido, J.-M. Fedeli, P. Rivallin, K. Surana, L. Pavesi Opto-electrical characterization of erbium-doped slot waveguides, Proc. SPIE 8431, Silicon Photonics and Photonic Integrated Circuits III, 843118 doi:10.1117/12.922695 (2012).
3. J. M. Ramirez, Y. Berencen, F. Ferrarese Lupi, D. Navarro-Urrios, A. Anopchenko, A. Tengattini, N. Prtljaga, L. Pavesi, P. Rivallin, J. M. Fedeli, B. Garrido, "Electrical pump & probe and injected carrier losses quantification in Er doped Si slot waveguides", *Opt. Express*, 20, 28808 (2012).

### 3. Infrared photoconductivity of Er-doped Si nanoclusters (Oleksiy Anopchenko)

Er-doped nanomaterials and photonic structures are of large interest because of their potential applications in integrated photonics and photovoltaics. Er ions coupled to Si nanoclusters is a promising optical gain medium of a waveguide amplifier and injection laser [1]. Er-doped dielectrics and semiconductors are used for photon up-conversion in advanced solar cells. Photonic structures are used to enhance light absorption and electronic transition rates in nanomaterials.

Silicon nanoclusters enable electrical excitation of Er ions [2] and present an attractive material for the next generation solar cells [3]. However, a role of the interface of nanoclusters in electrical and optical properties has not been yet completely understood. The presence of deep gap states, through which Si nanoclusters sensitize  $\text{Er}^{3+}$  ions, is a central point of several models of the energy transfer between Si nanoclusters and Er ions. Carrier multiplication and a considerable photocurrent due to the deep gap states were measured under sub-band gap illumination of a reverse-biased metal-oxide-semiconductor device with Si nanocrystals.

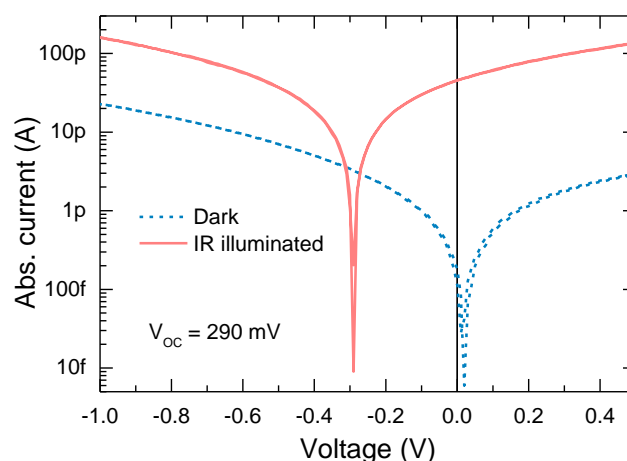


Figure 4. Current-voltage characteristics of the Er-doped SiOx waveguide in dark and under  $1.5 \mu\text{m}$  illumination (optical power  $\approx 7$  mW) bracketing 0 V and showing photovoltaic effect with the  $V_{oc} = 290$  mV. Voltage ramp rate is  $\leq 10$  mV/s.

Infrared photoconductive and photovoltaic effects have been observed in Er-doped Si nanoclusters in  $p-i-n$  slot-waveguide devices. The effects are ascribed to the presence of the deep gap states in silicon oxide due to the Si nanoclusters. The same states are believed to play a role of intermediate states in the sensitization of Er ions via Si nanoclusters. The room temperature open circuit voltage of the  $p-i-n$  device with Er-doped Si nanoclusters is 290 mV (Fig. 1) under monochromatic guided wave illumination with the photon energy (wavelength) of 827 meV ( $1.5 \mu\text{m}$ ). The light intensity exponent is found to take a value close to 0.5 and 1 for forward and reverse-bias conditions, respectively (Fig. 2). The former value is attributed to bimolecular recombination at the sub-band gap states (the

states are empty), and the latter is a characteristic of a linear recombination process with the deep gap states being populated with electrons.

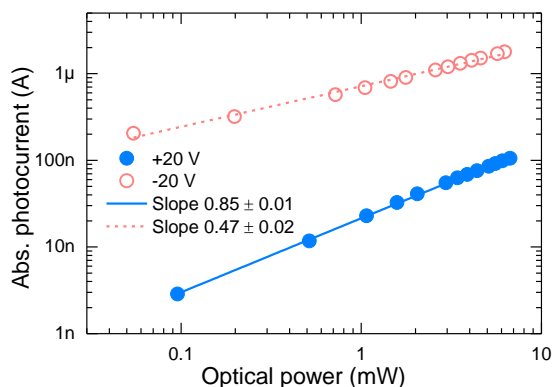


Figure 5. The absolute value of the photocurrent as a function of optical power incident on a waveguide grating coupler for two opposite electrical bias polarities. Lines are linear regressions through the experimental data points with the slopes indicated in the figure legend.

#### References:

1. A. Tengattini, D. Gandolfi, N. Prtljaga, A. Anopchenko, J. M. Ramirez, F. F. Lupi, Y. Berencen, D. Navarro-Urrios, P. Rivallin, K. Surana, B. Garrido, J. M. Fedeli, and L. Pavesi, "Toward a 1.54  $\mu\text{m}$  electrically driven erbium-doped silicon slot waveguide and optical amplifier," *Journal of Lightwave Technology* 31, 391-397 (2013).
2. A. Anopchenko, A. Tengattini, A. Marconi, N. Prtljaga, J. M. Ramirez, O. Jambois, Y. Berencen, D. Navarro-Urrios, B. Garrido, F. Milesi, J. P. Colonna, J. M. Fedeli, and L. Pavesi, "Bipolar pulsed excitation of erbium-doped nanosilicon light emitting diodes," *Journal of Applied Physics* 111, 063102 (2012).
3. Z. Yuan, A. Anopchenko, and L. Pavesi, "Innovative Quantum Effects in Silicon for Photovoltaic Applications," in *Advanced Silicon Materials for Photovoltaic Application* (John Wiley & Sons, Ltd, 2012), pp. 355-391.

#### 4. On-Chip Luminescent Biosensors based on Si-Waveguides. (Francisco J. Aparicio Rebollo)

Miniaturized and therefore portable lab-on-a-chip biosensors able to perform laboratory operations but on a small scale and to provide a real time response are very appealing for diverse fields, such as, point of care testing and food industry. Thanks to their high sensitivity, reliability, speed, and robustness, optical methods represent the most extended approach for the development of these biosensors. In this regard, Silicon Photonics is the preferred technology for on-chip applications since it allows to integrate at micrometric scale the different elements forming the optical transducer part (waveguides, beam splitters, multiplexing systems ...), and it is compatible with the other optoelectronic and microfluidic components present in a lab-on-chip biosensors. The research activity was focused on the design, fabrication and testing of a silicon waveguide optical biosensor. The operation principle is based on the fluorescent detection of intrinsically luminescent or fluorophore-tagged biomolecules. Thus, since the fluorescent emission can be detected with almost single-photon

resolution, it is virtually possible to detect the presence of a single tagged molecule.

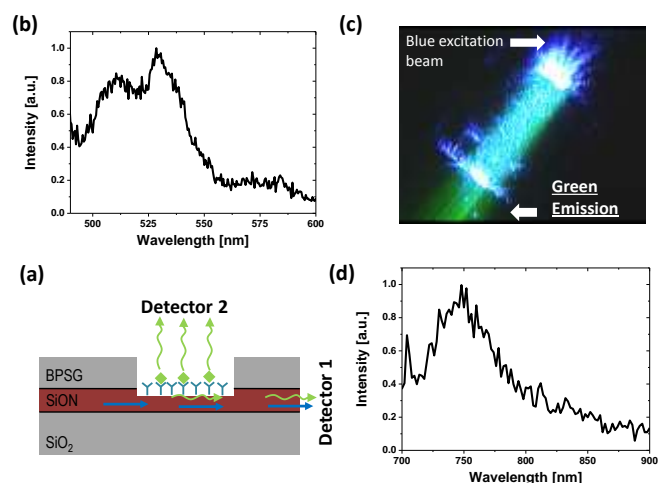


Figure 6. (a) Schematic side-view representation of the optical transducer at the bioreactor region. (b) Photoluminescence spectrum acquired from the top of a bioreactor (detector 2) with a surface concentration of 10-12 Moles/cm<sup>2</sup> 4<sup>2</sup>-(aminomethyl)fluorescein hydrochloride (AMF). (c) Microscopy image recorded from the top of a bioreactor infiltrated with a AMF solution. Excitation of the fluorescence emission is exclusively due to the laser beam propagating through the waveguide structure. (d) Photoluminescence spectrum at the waveguide's output (detector 1) in case of a bioreactor filled with a luminescent solution 10-4 M of Furescent Red 7000.

As illustrated in Figure 6a the photonic chip includes a micrometric (50 x 50  $\mu\text{m}$ ) bioreactor well that is functionalized with a bio-recognition layer for the selective immobilization of the target biomolecule. Design and dimensions of the optical transducer have been adjusted to excite the surface-immobilized biomolecules by the evanescent field of the waveguide modes. This approach assures the intense and uniform illumination of the bioreactor's bottom surface where the target biomolecules are trapped. The optical transducer can be used in two different configurations. In the transmission configuration (detector 1 in Figure 6a) the monitored signal corresponds to the fluorescence emission coupled back into the transmission waveguide by the evanescent field. Thus the fluorescence signal in Figure 6d is exclusively originating from those biomolecules trapped by biorecognition layer on bioreactor surface. In the second configuration, the SPAD photodetector (detector 2 in Figure 6a) is placed on top of the bioreactor well.[1] Besides its easy integration with the other device's components, this configuration allows using Si chips with multiple bioreactors carved in the same waveguide, an architecture that simplified the development of sensors arrays for multi-analyte sensing. In addition this configuration has been successfully used for the detection of a surface concentration of 10<sup>-12</sup> Moles/cm<sup>2</sup> of AMF (Figure 6b). Due to its low-cost mass production, the presented photonic chips are conceived as a disposable component of a modular-stack lab-on-chip microsystem also formed by a microfluidics delivery system and a silicon SPAD detector matrix.



**References:**

1 E. Rigo, F.J. Aparicio, M.R. Vanacharla, S. Larcheri, R. Guider, B. Han, G. Pucker, and L. Pavesi, "Evanescent-Field Excitation and Collection Approach for Waveguide Based Photonic Luminescent Biosensors" *Journal of Lightwave Technology*.  
 2 Francisco J. Aparicio, Eveline Rigo, Elena Froner, Silvia Larcheri, Marina Scarpa, Lorenzo Pavesi, Yoann Jestin and Georg Pucker, "Waveguide based Si photonic structures for a lab-on-chip biosensors" *Fotonica 2012*, Florence (Italy), May 2012.

**5. Integrated and mass-producible label-free biosensor (Davide Gandolfi)**

Biological analyses are conducted in specialized laboratories with very sensitive but expensive and bulky equipments. At the same time, point-of-care analysis would need compact and yet sensitive biosensors, able to produce a response in a short time.

Within this framework, silicon photonics has proven to be a valuable tool: it can be mass-produced and it is based on micrometric-sized elements. To enhance the interaction between the lightwave and the analyte, the use of optical resonators is particularly appealing.

In the Nanoscience Laboratory, we propose and investigate the use of vertically coupled whispering gallery mode (WGM) resonators. With this choice, the buried waveguide and the coupling region are protected and not exposed to the sample fluid.

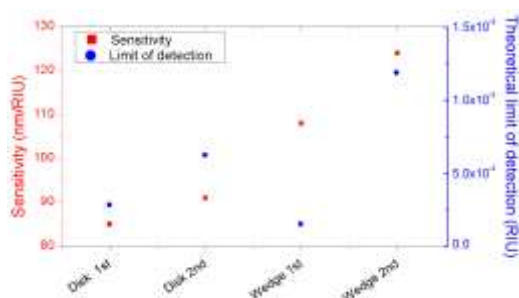


Figure 7. Comparison of the performances for the first and second radial mode family in the two resonator geometries. Compared parameter are the sensitivity (red, left) and of the limit of detection (blue, right).

We tested and compared two different resonator geometries, namely the disk and the wedge resonator [1]. The latter, in particular, showed superior performances, both in terms of sensitivity and quality factor, which in the end led to a better limit of detection.

Specific sensing of Vascular Endothelial Growth Factor (VEGF165) proteins was performed on a wedge resonator. Aptamers were chosen as specific bio-recognition agents and immobilized on the surface of the WGM resonator [3,4].

The tests were performed with buffered protein solutions of known concentration. A drop of these solutions was left on the functionalized resonator for a fixed amount of time (incubation). The resonance shifts have been measured as a function of the incubation time and of the protein concentration.

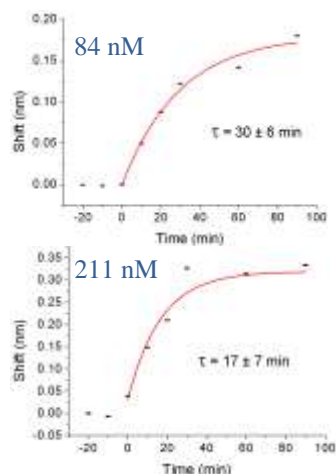


Figure 8. Binding reaction kinetic measurements. The resonance shift is measured as a function of the incubation time for two different known protein concentrations (84 and 211 nM).

The clear exponential dependence of the shift with the incubation time (figure 8) is a measurement of the protein-binding reaction kinetic. By measuring the time constant it is possible to estimate the protein concentration.

**References:**

1 F. Ramiro-Manzano et al. "A fully integrated high-Q Whispering-Gallery Wedge Resonator", *Opt. Express*, 20, 22934 (2012)  
 2 L. Pasquardini et al., "Whispering gallery mode aptasensors for detection of bloodproteins", *Journal of Biophotonics*, 6 (2) p. 178-87  
 3 S.D. Jayasena, "Aptamers: an emerging class of molecules that rival antibodies in diagnostics", *Clin. Chem.*, 45(9), p. 1628-50, (1999)

**6. Synthesis and characterization of hybrid materials (Paolo Bettotti)**

In recent years, research activities at NL encompass material science topics that investigate the use of hybrid material for optoelectronic and analytical applications. Because of their interdisciplinary nature most of these themes are collaborations among different research groups. The three main topics are briefly described below:

1. Characterization of growth mechanism and optoelectronic properties of organic semiconductors. Within a long term collaboration with Dr. T. Toccoli of CNR-IMEM centre, NL exploits its knowledge in Scanning Probe Microscopy to characterize the mechanisms of growth of organic semiconducting molecules. AFM measurements on samples deposited by the CNR group demonstrate how the growth methods of acenes molecules depends on the deposition conditions and from the surface properties (wettability). NL also perform optical characterization of such compounds with the aim to realize innovative and efficient Light Emitting Devices.

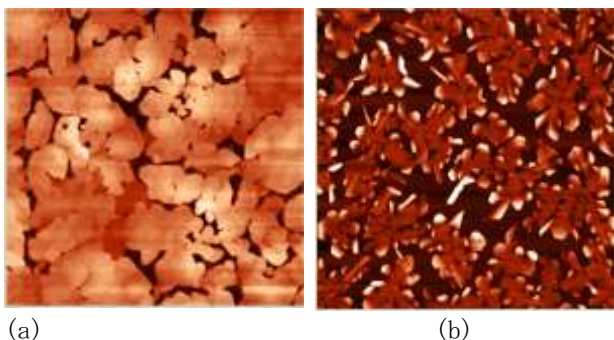


Figure 9. (a) pentacene islands (image size 10 x 10  $\mu\text{m}$ ), (b) picene crystals (image size 15 x 15  $\mu\text{m}$ )

2. Silicon nanocrystals are efficient light emitters and are actively studied as bio-compatible fluorophores. Since several years, NL was producing Si-nc from Porous Silicon. Recently we investigate chemical synthesis based on more “clean” and reproducible protocols to obtain such nanoparticles. Among the different receipts described so far in literature, one of the most effective method is based on sol-gel synthesis starting from pure chlorosilane reagents. Once created the non stoichiometric SiO<sub>x</sub> gel, the silicon nanoparticles form after a thermal treatment performed in reducing atmosphere. Bright luminescent solutions containing large amount of Si-nc are thus created. The Si-nc will be used to dope optical fiber within a collaboration with the Institute of Advanced Photonics of the Univ. of Adelaide.

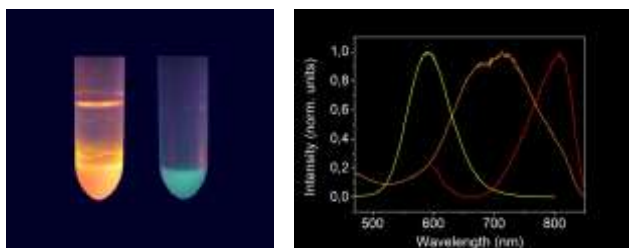


Figure 10 Picture of solutions containing Si-nc under UV illumination. The different colours result from different nanocrystal sizes.

#### Acknowledgments:

This theme is supported by the Provincia Autonoma di Trento through the Nano@AT project.

3. The NL expertise on Porous Silicon and the collaborations established in European research networks have led to the successful evaluation of a project proposal within the FIRB-Futuro in Ricerca program. This project will start in 2013 and its aim is to study the diffusion and the reactivity of biological materials in nanoconfined systems. More info at:

<http://www.science.unitn.it/~semicon/members/bettotti/numeric/>

#### References:

"Optimizing Picene Molecular Assembling by Supersonic Molecular Beam Deposition", S. Gottardi, T. Toccoli, S. Iannotta, P. Bettotti, A. Cassinese, M. Barra, L. Ricciotti, Y. Kubozono, J. Phys. Chem. C, 116, 24503 (2012)

## 7. Organic vapor sensing with free standing N-type porous Silicon Microcavities (Neeraj Kumar)

Porous Silicon (PSi) is an ideal candidate material because it is compatible with both technological and biochemical aspects [1]. Till date several PSi based devices remain attached to the bulk-silicon substrate and this flow-over geometry shows several drawback to develop efficient and sensitive analytical tools. P-type silicon substrate allows the fabrication of free-standing membranes but this substrate suffers of two important limits: etched porous sponges are limited to small pore size the render difficult or impossible to infiltrate (or filter) large bio-molecules. N-type PSi structures provide an alternative with compatible and even larger pore size for sensing of bio-molecule. A seminal report about the possibility to use n-type substrates for sensing is where the authors demonstrate bio-sensing in n-type PSi MC on silicon substrate. Further, a highly sensitive optical transducer mechanism based on a phase interrogation readout scheme for the anisotropy characterization of mesoporous silicon membranes could be another approach. But samples of interest for real application often require the fabrication of very thin porous membranes, thus high quality etching has to be engineered and this approach is limited by the impossibility to fabricate n-type freestanding microcavity MC or membrane porous structure.

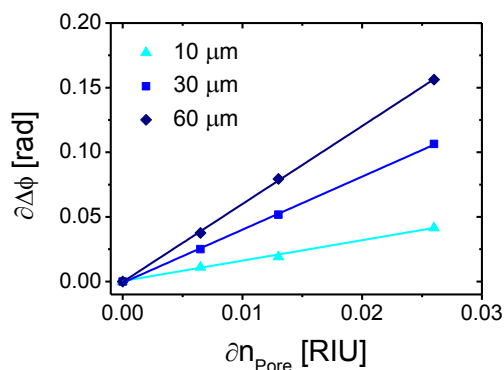
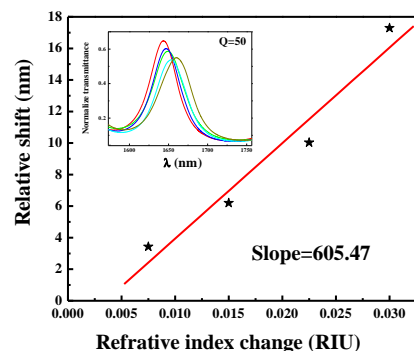


Figure 10. Resonance shift of MC after expose to various concentrations of ethanol and linear fit. Phase retardation shifts for samples rotation angle of 45° as a function of the refractive index of the material filled in pores for 10  $\mu\text{m}$ , 30  $\mu\text{m}$  and 60  $\mu\text{m}$  (dots).

PSi n-type (0.01-0.02  $\Omega\text{cm}$ ) multi-layer MC structures were prepared by electrochemical etching method using a solvent containing 12.5% v HF by volume in de-ionized

water and detached with 12%v HF in ethanol with 23% $H_2O_2$  solution. MCs were fabricated using alternating current density of 40 mA/cm<sup>2</sup> for 9.26 sec and 80 mA/cm<sup>2</sup> for 8.14 sec, respectively, for the higher refractive index (2.2) and the low refractive index (1.7). MCs of different quality factor (Q=30, 50 and 70) were fabricated depending on the number of periods (i.e. 10, 14 and 20 layers). Pore diameter observed from SEM image for these MCs was 40nm and 110nm for the two layers that is sufficient for any latex infiltration. Figure 10 shows the shifts in resonance due to an increase in refractive index as liquid fills the pores. Shifts of ~186.3nm, 194.7nm and 200nm are observed when MCs of Q=30, 50 and 70 are exposed to methanol. These correspond to a sensitivity of about 565nm, 590 and 606nm RIU<sup>-1</sup>. MC with Q=30 and Q=50 shows a shift 13.18nm and 17.29nm due to change in refractive index ( $\Delta n = 0.03$ ), when methanol is exchanged with ethanol. As slope of shift points indicates the sensitivity of photonic structure due to change in refractive index, sensitivities  $\sim 2.06$ ,  $1.65 \cdot 10^{-4}$  and 1.5 are calculated with the resolution limit of optical instrument (0.1nm). Furthermore, these free-standing MC structures can be used in active flow-through bio-sensor and are under study.

Further for optical transducer approach, PSi membranes with thickness of 10, 30 and 60  $\mu m$  were fabricated. The birefringence was measured by means of measuring the phase retardation as a function of the light incidence angle with a resolution of  $10^{-7}$  rad [2]. Immersing freestanding membranes in several solutions of water and ethanol, it is observed that thicker membranes present higher sensitive values. Side by side as the membrane thickness increases also the depolarization does, which deteriorates the resolution in the phase retardation measurement. Combining the sensitivity and the resolution results, we obtained that the thinnest membrane (10  $\mu m$ ) presents the higher limit of detection, being equal to  $6.25 \cdot 10^{-6}$  RIU and high thermal stability with a thermo-optic coefficient of  $8 \cdot 10^{-4}$  rad/RIU. Linear fitting to experimental data shows sensitivities of 1.5 rad/RIU and 4.5 rad/RIU for the 30  $\mu m$  and 60  $\mu m$  thick respectively. As these membranes have pores diameters around 50 nm and are suitable for the infiltration of biomolecules, these freestanding porous layers could be actively used for biosensing with low limit of detection.

This work was supported by the European Commission through the project FP7-257401 POSITIVE.

## References

1. J. Alvarez, P. Bettotti, I. Suarez, N. Kumar, D. Hill, V. Chirvony, L. Pavesi, J. Martinez-Pastor, *Opt. Express*, 19, 26106 (2011)
2. J. Alvarez, N.Kumar, P. Bettotti, D. Hill and J. Martinez-Pastor, *Photonics journal IEEE*, 4, 986 (2012)

## 8. Porous silicon micropowder for drug delivery (Elena Froner, Paolo Cortelletti, Marina Scarpa)

The aim of this project is to study the influence of the immune response system, in particular of macrophages, on the development of colorectal cancer (CRC) by trying to manipulate the macrophages phenotypes themselves. The role of our laboratory is to design and set up luminescent

nanoporous silicon microparticles able to deliver a specific kind of drug molecules, small interfering RNA (siRNA), to the tumor associated macrophages (TAM). When a specific siRNA enters the TAM membrane, it can lead the cell to the expression of an antitumoral phenotype. A drug delivery vector is required to bring the siRNA safe to the macrophages. Porous silicon microparticles are expected to be a perfect vector, as they are obtained from porous silicon disruption by sonication, they should allow high siRNA loadings inside the pores, they seem to be biocompatible (as they are degraded into silicic acid with rates depending on their chemical and morphological characteristics). We have obtained porous silicon microparticles in the range 3-10  $\mu m$  with pore diameter of the order of 20 nm (see Fig. 11).

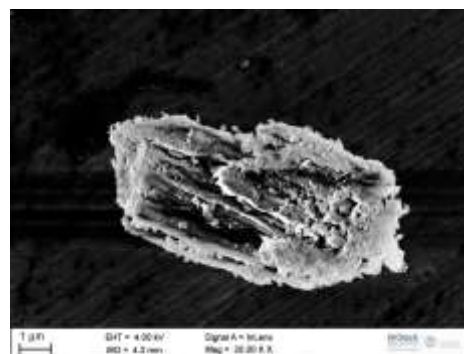


Figure 11. SEM image of a diamine functionalized Silicon microparticle

The microparticles have been functionalized by a wet procedure to introduce carboxylic groups. These groups have been coupled to diamines to obtain a positively charged surface (see Fig. 12 where we show the IR spectra of the functionalized microparticles). We have now preliminary data which demonstrate that the microparticles can be loaded with molecules bearing negative charges (as siRNAs) and the payload is slowly released in solutions which simulate the body fluids.

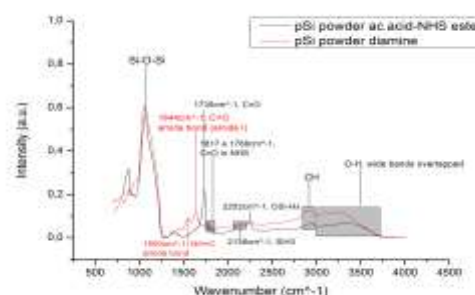


Figure 12. FTIR spectrum of silicon microparticles functionalized by the NHS ester of the acrylic acid and by amines.

## 9. Titanate nanostructures for drug delivery and photocatalysis (Elena Froner and Marina Scarpa)

Nanotubes derived from  $TiO_2$  are attracting increasing interest because of their peculiar properties such as a high aspect ratio, a mildly reactive nature of their surface, and

the semiconductor band gap that can be tuned from UV to visible range. In particular, titanate nanotubes are excellent photocatalysts able to oxidize toxic organic compounds when added to contaminated water and illuminated by mild UV light. This is a clean process for contaminant removal since, besides atmospheric oxygen, no other reagent is needed for the reaction to proceed. Up to now the majority of the experimental proofs of the  $\text{TiO}_2$  nanotube performances have been obtained using  $\text{TiO}_2$  nanotube assemblies, or layers or powders dispersed in solvents. We have set up a procedure to obtain stable and concentrated  $\text{TiO}_2$  nanotube aqueous solutions. Morphological characterization of these soluble  $\text{TiO}_2$  nanotubes has been performed. The relationships between solubility, structure and solvent exposed interface, i.e. the presence of surface sites where  $\text{Na}^+$  ions are confined, have been investigated by means of optical and vibrational spectroscopies and, also, by solution Nuclear Magnetic Resonance.

### 10. Measuring disorder with the Coupled Resonator Induced Transparency concept (Massimo Borghi)

Silicon On Insulator (SOI) integrated photonic devices suffer from nanometre scale imperfections due to the inherent resolution limits of the photolithography and etching processes. This dictates limitations in reproducibility and reliability, especially in high phase sensitive structures for DWDM applications like sequences of microring resonators. It would be important to have a simple tool that allows a control of the disorder level directly on wafer, without the need of advanced analysis techniques like CD-SEM or ellipsometry. The Side Coupled Integrated Spatial Sequences of Resonators (SCISSOR) [1] geometry is very sensitive to fabrication errors, since the lack of periodicity in the resonator chain gives rise to Coupled Resonator Induced Transparency states in the stop band, that manifest themselves as high Q transparency peaks. Our idea was to exploit the strong correlation between CRIT and defects to develop a quick, simple and all optical method to extract informations about the disorder distribution. We experimentally characterized the CRIT effect from many nominally identical SCISSORs, and we compared the results with computer simulations. We found a so strong correlation that only a very limited set of the simulated defects distributions are compatible with the observed data. The fluctuation of the resonator radius has been observed to play the most important role and has been estimated with a relative error below the 12%. This means that SCISSORs are good candidates for probing the disorder distribution, and led us to propose a new test structure that speeds up the whole estimation process. The device geometry is shown in fig.13. It consists of a series of  $N_c$  SCISSORs, each made by  $N_r$  resonators. Values of  $N_r$  and  $N_c$  has to be found as a tradeoff between sensitivity and footprint. This configuration sums up the CRIT defect states of each SCISSOR. The result is that the photonic band in the Out port misses from the power of the CRIT states, and presents instead several dips. As the magnitude of defects increases, number and width of the dips also becomes higher. Briefly, the Out power, normalized with respect to the Ref port, is an

indicator of how much the resonator radii locally fluctuate on the device area.

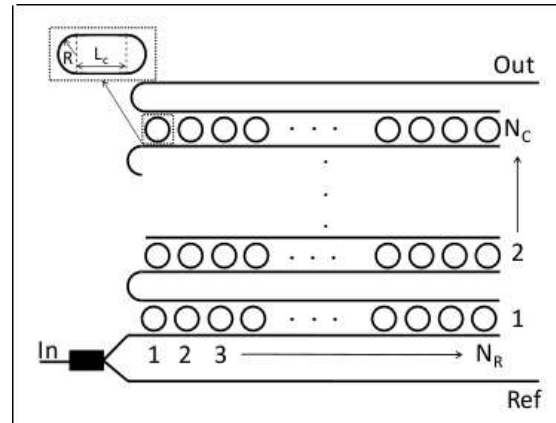


Figure 13: Schematic of the test structure. It has three ports, the In, the Ref and the Out. Resonators can be either rings or race-tracks.

Figure 14(a) reports the design for a  $N_r = 14$ ,  $N_c = 10$  test structure. It uses a broadband source (i.e an ASE source), as input. Two input-output gratings inject and collect light from two single mode optical fibers. The error estimation process is done by aligning the fibers and, then, measuring the ratio between the Out and the Ref port. This value has to be compared with the pre-calibrated curve in figure 14(b), that yields an estimation of the resonator radius fluctuation (in terms of its standard deviation) together with the relative accuracy.

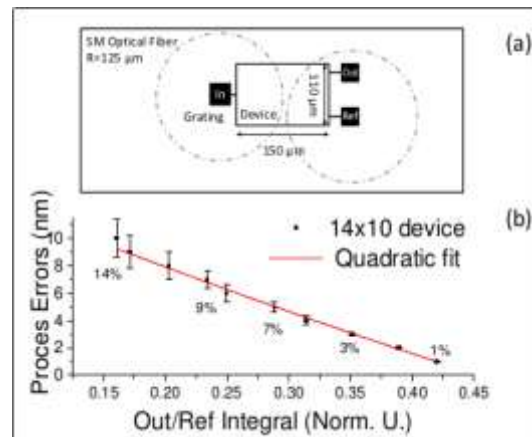


Figure 14. (a) A device sketch. (b) Calibration curve for the  $N_c = 10$ ,  $N_r = 14$  device showing the value of the Out/Ref value as a function of the ring radius variations (standard deviation). Percentage values indicate the relative error of the estimation.

In conclusion, our proposal offers a quick, simple and non-invasive method to quantify the disorder level on a chip with accuracy below 14%. The device is particularly suitable for being applied in post process wafer defects control

### 11. Monolithic integration of high-Q wedge resonators with vertically coupled waveguides (Fernando Ramiro Manzano)

Whispering gallery mode microresonators with ultra-high quality factors (UHQ's) have attracted great attention because of their importance for fundamental science and potential applications. However, typical UHQ resonators, such as microspheres and microtoroids, lack the possibility of integration into lightwave circuits due to their planarity constrains. For this reason, the improvement of the quality factors of planar resonators fabricated using conventional semiconductor processing has provoked significant interest. In this context, CMOS-compatible alternatives in the form of wedge resonators have been proposed. In such a cavity geometry, the fundamental modes are pulled away from the resonator's periphery reducing significantly the surface-induced scattering losses. In fact, a new benchmark of UHQ on a chip has been set by using silica wedge resonators. However, the mode retraction from the cavity inhibits the possibility to side couple with integrated waveguides and therefore, halts the full integration within a planar lightwave circuit (see Fig 15). We have demonstrated the feasibility of a full integration of wedge resonators and bus waveguides by employing a vertical-coupling strategy [1]. In this approach, the resonator and the waveguide lay in different planes, which permits to realize the optical components in independent and isolated technological steps.

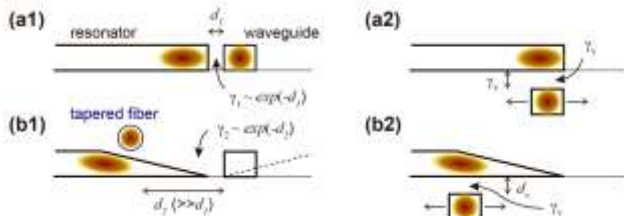


Figure 15 Schemes of the evanescent field coupling in integrated disk (a) and wedge resonators (b). The coupling rate  $\gamma$  imposes a nanometric gap between the resonator and the waveguide (a1, a2). In the case of the wedge resonators, the retracted mode limits the in-plane coupling (b1) and, therefore, off-chip techniques based on tapered-fibers are typically used. The vertical-coupling strategy allows tuning the vertical and horizontal distance for accessing to the retracted mode.

As a result, the waveguide remains intact when the wedge geometry of the cavity is formed. Owing to the fact that the vertical coupling gap is accurately controlled through a deposition procedure, the lithographic techniques employed are conventional and inexpensive. Advantageously, the vertical coupling scheme permits to select different materials for the resonator and the waveguide. Moreover, the gap material can be selectively removed in order to form freestanding wedge resonators extending the material and application ranges. These features are highly valuable for a number of applications such as cavity optomechanics, non-linear optics, label-free sensing and integrated photonics. In conclusion, the vertical-coupling scheme allows a full integration of wedge resonators on a chip featuring ar-

bitrary gaps, geometries and materials, enabling simplified and precise control of the light injection into the cavity and opening the door to an industrial mass-fabrication of UHQ resonators.

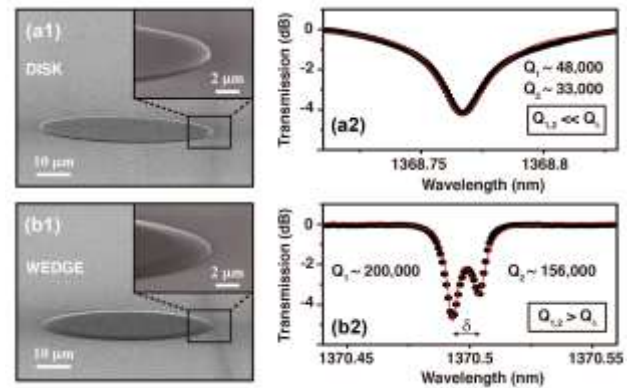


Figure 16. SEM images of disk (a1) and wedge (b1) vertically coupled resonators. Panels (a2) and (b2) represent the normalized waveguide optical transmission spectra of a disk and wedge resonators respectively. Lorentzian fits (red lines) to the experimental data (black points) reveals about a fourfold Q-enhancement of the wedge with respect to those of the disk.

#### References:

1. Ramiro-Manzano, F., Prtljaga, N., Pavesi, L., Pucker, G. and Ghulinyan M. Opt. Express, 20, 22934-22942 (2012).

### 12. A further investigation of the second order nonlinearity of strained silicon waveguides (Federica Bianco)

Thanks to the tight confinement of the light in silicon sub-micron-structures and the high nonlinearity of silicon, the nonlinear silicon photonics is a relevant branch of silicon photonics for the development of novel active devices on the chip scale. Despite of the high variety of nonlinear effects, silicon lacks the second order nonlinearity, which is an essential component of nonlinear optics. In fact, by means of second order nonlinear phenomena new spectral components could be generated, for example, in the mid- and far-infrared via different frequency generation. In addition, the exploitation of the Pockels effect would allow the electro-optical modulation and, thus, the fabrication of silicon-based modulators that do not suffer from the limitations imposed by the carriers-related speed.

In our previous work [1], we have demonstrated the possibility to induce a  $\chi^{(2)}$  of several tens of picometers per volt by inhomogeneously straining silicon waveguides by means of deposition of stressing silicon nitride claddings. The second order nonlinear response of such structures has been studied carrying out second-harmonic-generation (SHG) experiments, which have revealed a  $\chi^{(2)}$  values dependence on the inhomogeneity and extent of the strain. Recently, we have performed a further study of the induced second order susceptibility in strained silicon waveguides and investigated the role of interface and stress-induced contributions by making use of samples fabricated with different materials (silicon nitride and silicon oxide) and covering configurations (top and completely covering), as shown in Fig. 17.

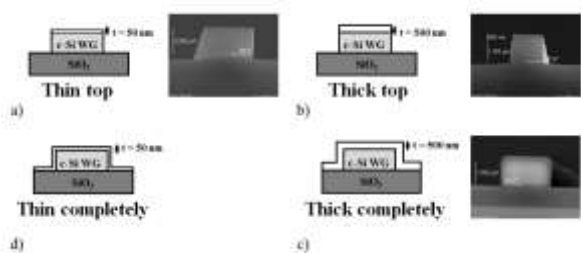


Figure 17. Samples classification: a-b) sketches and relative SEM images (silicon nitride layer) of top covering configuration with a thin (50 nm-high) or thick (500 nm-high) stressing layer; c-d) sketches and relative SEM images (silicon nitride layer) of completely covering configuration with a thin (50 nm-high) or thick (500 nm-high) stressing layer.

This new study of the second order nonlinearity has been accomplished through the analysis of the conversion efficiencies measured in new SHG experiments. The pure stress-related effect in the second order nonlinear properties has been confirmed by the comparison between waveguides covered by the native oxide and a stressing layer of silicon oxide. Instead, waveguides covered by silicon nitride layer with negligible stress have surprisingly shown a conversion efficiency comparable to the one measured in the sample covered by the stressing silicon oxide layer. This result has revealed a significant surface effect originating from the interface between silicon and silicon nitride, whose origin is not yet clear. Nevertheless, in presence of silicon nitride layer exerting a stress on the underlying waveguide, an increase of the conversion efficiency has been observed, as shown in Fig. 18. This result has indicated that in waveguides strained by silicon nitrite the second order nonlinearity has origin from the superposition of interface and strain effects.

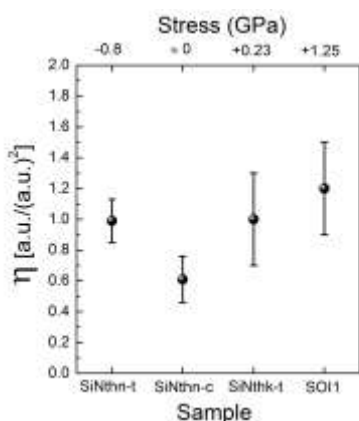


Figure 18: Study of the conversion efficiency enhancement due stress-induced effects in 10  $\mu\text{m}$ -wide waveguides. *SiNthn-t* refers to the sample where a 50 nm-thick silicon nitride overlayer covers the top surface of the waveguide and applies a stress of -800 MPa; *SiNthn-c* is the sample where the waveguides are completely covered by a 50 nm-thick silicon nitride layer with negligible stress; *SiNthk-t* is the sample where a 500 nm-thick silicon nitride overlayer covers the top surface of the waveguide and applies a stress of +226 MPa; *SOI1* is one of the 2 mm-long samples used in the first SHG experiment, where a 150 nm-thick silicon nitride

overlayer covers the top surface of the waveguide and applies a stress of +1.25 GPa.

Work in collaboration with the SiLi-nano Group from Martin Luther-University (Halle-Wittenberg, Germany).

### References

1. M. Cazzanelli, F. Bianco, E. Borga, G. Pucker, M. Ghulinyan, E. Degoli, E. Luppi, V. Vénard, S. Ossicini, D. Modotto, S. Wabnitz, R. Pierobon and L. Pavesi, "Second-harmonic generation in silicon waveguides strained by silicon nitride", *Nature Materials* **11**, 148-154 (2012).

### 13. Racetracks based reconfigurable optical interleaver (Mattia Mancinelli)

Wavelength Division Multiplexing (WDM) requires interleaver (IL) with dense channel spacing to route a large number of signals along the network. Most of the proposed interleavers has a large footprint and their performance is heavily affected by fabrication errors, thus they require a post-fabrication trimming process.

Here, we experimentally demonstrate a novel reconfigurable optical band IL that is robust against fabrication defects, has small footprint and competitive performances. Fig. 18(a) shows the CROW based band interleaver (BIL) that is used to achieve band routing. Fig. 1(b) shows the single resonator IL, which, is used to divide the entire spectral window into several sub-bands (SBs).

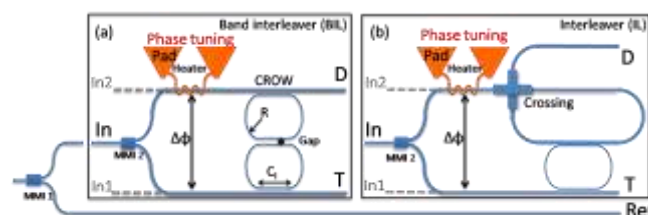


Figure 18. (a) Design of the (a) reconfigurable band interleaver and (b) reconfigurable interleaver. Photonic layer (blue): interferometric device composed of an input channel (In) or two inputs (In1 and In2, grey) and two outputs: the T and the D ports. The Reference (Ref) is used to normalize the data. MMIs are 50/50 splitters. The metallic heater is shown in orange: it is used to induce a  $\Delta\phi$  on one arm of the device. See text for other symbol explanation.

Using interferometry, the usual Add/Drop filter is transformed into either a 4 or a 3 ports device. The 4 ports device has two inputs (In1, In2) and two outputs (T,D) (Fig. 18 dashed grey lines). The In2 port is used as input for a second signal, coherent to that of the In1 port, which interferes inside the CROW sequence. Depending on their phase relation and wavelength the two signals are routed in either one of the two output ports or in both ports. The 3 port device has only one input (In1=In2=In) and two outputs (T,D). The signals are equally divided and fed into the In ports by the MMI2. The phase difference ( $\Delta\phi$ ) between the two light paths is ruled by a heater (drawn in orange in Fig. 18 and are recombined by the CROW (Fig. 18(a)) or by the single resonator (Fig. 18(b)). Figure 19(a) shows the transmission of T port of a IL composed by 4 resonators.

The bands, highlighted by the grey rectangles, are spaced by a free spectral range (FSR).

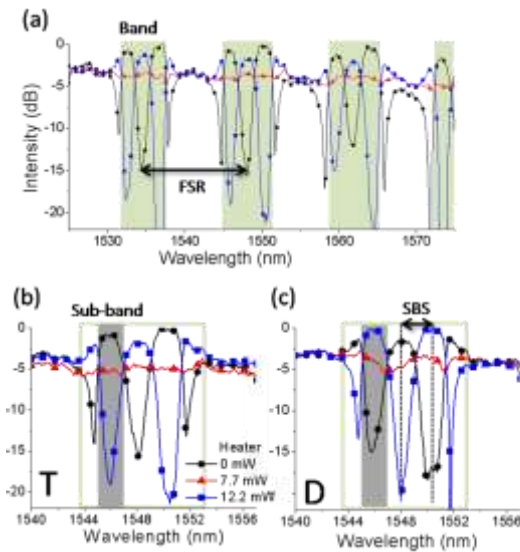


Figure 19. (a) Transmission spectra of the T port for several resonance order. The bands are high-lighted by the green rectangles. Transmission spectra of the (a) T port and (b) D port for several powers dissipated by the heater: 0 mW (black), 7.7 mW (red), 12.2 mW (blue) corresponding to a  $\Delta\varphi$ , respectively, of  $0\pi$ ,  $\pi/2$ ,  $\pi$ . The SBs are highlighted by the grey rectangles.

Figures 19 (b,c) show a high resolution spectra of a single band for the T and D ports for different  $\Delta\varphi$ . Let us concentrate on the single SB, highlighted by the gray area: for  $\Delta\varphi = 0$  (black line) the signal is routed to the T port while for  $\Delta\varphi = \pi$  (blue line) the signal is routed to the D port. A new functionality is observed for  $\Delta\varphi = \pi/2$  (red line): for this phase difference the signal is split equally between the two output ports.

Our proposed designs are examples of more complex structures where both wavelength and phase differences can be used to implement complex networking protocols.

#### 14. Silicon Nanocrystals for Photovoltaic Applications (Fabrizio Sgrignuoli)

Silicon nanocrystals (Si-NCs) are interesting material for photovoltaic applications. Their implementation on silicon based solar cells can reduce the loss mechanisms produced by a poor conversion of the UV-incident photons thanks to the luminescent downshifting effect (LDS). An high energy photon is absorbed while a low energy photon is emitted by Si-NCs, increasing the number of carriers photo-excited effectively used by the solar device.

Two different fabrication methods have been developed within the European project LIMA to exploit the LDS effect:

- Integration of Si-NCs during the fabrication process of interdigitated back contact (IBC) solar devices;
- Integration of this novel layer after the fabrication of IBC cells.

In both approaches, an improvement of the short circuit current density by using Si-NCs is measured with respect to a reference IBC solar device. The enhancement, obtained following the first method, was attributed to a com-

ination of LDS effect and a better surface passivation. Using the second method, we enucleated only the LDS effect demonstrating the role played by Si-NCs in the increased performances.

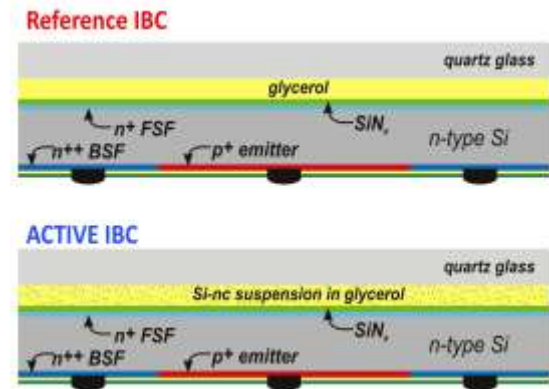


Figure 20. Method used to integrate Si-NCs after the fabrication process of IBC solar cells. The reference (top) and the ACTIVE IBC (bottom) are characterized by glycerol and colloidal Si-NCs in glycerol solution respectively in the quartz-cover/IBC spacing layer.

A schematic representation of the method used to integrate Si-NCs after the IBC fabrication process is illustrated in the fig. 20. The same IBC solar cell is used in the reference and active configuration characterized respectively by glycerol and colloidal Si-NCs in glycerol solution in the quartz-cover/IBC spacing layer. In the active configuration an improvement of the short circuit density up to 1% was measured with respect to the reference (see fig. 21 a). This increase is due to LDS effect since the cell are exactly the same in the performed experiment and their surface is coated with liquids that shows the same “passive“ optical properties (see fig. 21 b). Simulation reproduces with well the experimental results considering a quantum efficiency of the nanocrystals of 30%, which was independently confirmed by experimental measurements.

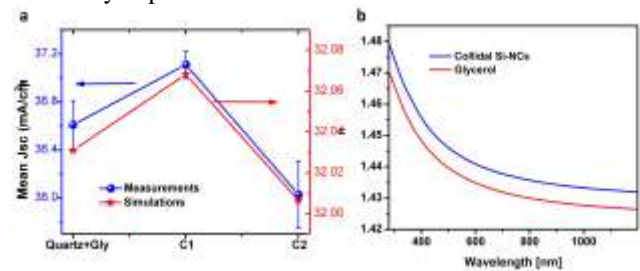


Figure 11. a) Short circuit current density for the reference and active configuration (red lines). C1 and C2 refer to colloidal Si-NCs with different concentrations. The drawn blue line identifies the simulations performed using the method described in [1]. b) Real part of the refractive index of colloidal Si-NCs (blue) and glycerol (red) solution measured by using a variable angle spectroscopic ellipsometer. The “passive“ optical properties of the used solutions are the same excluding a possible enhancement thanks to a better optical matching.

#### References:

1. F. Sgrignuoli, G. Paternoster, A. Marconi, P. Ingenhoven, A. Anopchenko, G. Pucker, L. Pavesi, J. Appl. Phys., 111, 034303 (2012)

**For more info**

Nanoscience Laboratory  
Physics Department - Science Faculty  
University of Trento  
via Sommarive 14  
38123 Povo- Trento (Italy)  
<http://www.unitn.it/en/dphys/7421/nanoscience>  
<http://science.unitn.it/~semicon/>

secretary dr. Tatsiana Yatskevich  
email [tanya@science.unitn.it](mailto:tanya@science.unitn.it)  
phone +390 461 283172  
fax +390 461 282967